Earth and Planetary Science Letters 477 (2017) 73–83

Contents lists available at ScienceDirect

Earth and Planetary Science Letters

www.elsevier.com/locate/epsl

The role of unsteady effusion rates on inflation in long-lived lava flow fields

E. Rader [a,*], L. Vanderkluysen [b], A. Clarke [c]

[a] NASA Ames Research Center, United States
[b] Drexel University, United States
[c] Arizona State University, United States

ARTICLE INFO

Article history:
Received 25 January 2017
Received in revised form 9 August 2017
Accepted 12 August 2017
Available online xxxx
Editor: T.A. Mather

Keywords:
flood basalt
inflation
eruption tempo
lava morphology
large igneous province
lava flows

ABSTRACT

The emission of volcanic gases and particles can have global and lasting environmental effects, but their timing, tempo, and duration can be problematic to quantify for ancient eruptions where real-time measurements are absent. Lava flows, for example, may be long-lasting, and their impact is controlled by the rate, tempo, and vigor of effusion. These factors are currently difficult to derive from the geologic record but can have large implications for the atmospheric impact of an eruption. We conducted a set of analogue experiments on lava flow inflation aiming at connecting lava morphologies preserved in the rock record to eruption tempo and dynamics through pulsating effusion rates. Inflation, a process where molten material is injected beneath the crust of an active lava flow and lifts it upwards, is a common phenomenon in basaltic volcanic systems. This mechanism requires three components: a) a coherent, insulating crust; b) a wide-spread molten core; and c) pressure built up beneath the crust from a sustained supply of molten material. Inflation can result in a lava flow growing tens of meters thick, even in flow fields that expand hundreds of square kilometers. It has been documented that rapid effusion rates tend to create channels and tubes, isolating the active part of the flow from the stagnant part, while slow effusion rates may cause crust to form quickly and seize up, forcing lava to overtop the crust. However, the conditions that allow for inflation of large flow fields have not previously been evaluated in terms of effusion rate. By using PEG 600 wax and a programmable pump, we observe how, by pulsating effusion rate, inflation occurs even in very low viscosity basaltic eruptions. We show that observations from inflating Hawaiian lava flows correlate well with experimental data and indicate that instantaneous effusion rates may have been 3 times higher than average effusion rates during the emplacement of the 23 January 1988 flow at Kīlauea (Hawai'i). The identification of a causal relationship between pulsating effusion rates and inflation may have implications for eruption tempo in the largest inflated flows: flood basalts.

1. Introduction

1.1. Flow emplacement, eruptive process, and environmental impact

The hypothesized environmental impact of eruptions greater than 100,000 cubic kilometers (such as the flood basalts of the Deccan and Siberian traps) is in part controlled by the tempo of eruptive pulses (Courtillot and Fluteau, 2014; Black and Manga, 2017; Tobin et al., 2017). The tempo of an eruption is a term used to capture the duration of effusion rate of individual pulses of high flux as well as the time between those pulses, which often occurs in a periodic manner. The proposed relationship between eruption tempo and environmental impact emphasizes the importance of constraining the rate and unsteadiness of large inflated lava flows. Sufficiently large gas emissions can overwhelm the atmosphere's ability to respond, and can thus have substantial global warming and ocean acidification implications (Black and Manga, 2017). While the rate at which gas was released in these ancient eruptions is unknown, the rate of gas release is tied to effusion rate, which controls lava flow emplacement, including surface morphology, total duration, and area covered. Our ability to understand eruption dynamics and their environmental impacts thus depends on our understanding of the link between the dynamics of lava flow emplacement and their preserved deposits.

* Corresponding author.
E-mail address: Erika.rader@nasa.gov (E. Rader).

http://dx.doi.org/10.1016/j.epsl.2017.08.016
0012-821X/

1.2. Lava flow morphology and vertical growth

An active lava flow can be divided into three parts: the cool brittle crust, the flexible viscoelastic transition zone, and the molten interior that is surrounded on all sides by the other two zones (Castruccio et al., 2013 and references therein). The morphology of a lava flow is determined by the thickness and flexibility of the surface crust and the degree to which it is coupled to the molten interior of the flow (e.g., Cañón-Tapia et al., 1997; Cashman et al., 1999; Duraiswami et al., 2003). Crust that is coupled with the core of the flow (typically higher viscosity lava) will result in a lava flow that is either forced to thicken by flowing on top of itself or is torn apart by the shearing force between the molten interior and the rigid crust, resulting in a disjointed morphology like ʻaʻā, spiny or slabby pāhoehoe, and blocky lava (Peterson and Tilling, 1980; Pinkerton et al., 2002). A solid crust decoupled from the molten interior, however, remains intact while the molten material passes below. Smooth surface morphology is preserved in a coherent insulating crust, which allows new lava to be injected beneath it (Hon et al., 1994; Self et al., 1997; Anderson et al., 1999; Cañón-Tapia and Coe, 2002; Reidel et al., 2013). Rapid instantaneous flow rates of lava typically lead to strong coupling and therefore broken, rubbly-crusted or channelized flows whereas lower flow rates lead to decoupling and are correlated with the formation of smooth pāhoehoe crust (Rowland and Walker, 1990). Slow instantaneous effusion rates are also correlated with lower heat input and faster cooling rates, which will create flows consisting of numerous lobes, piled on top of each other and locally resurfacing the flow when subcrustal pathways solidify and become blocked (Moore, 1975; Griffiths and Fink, 1992; Keszthelyi and Denlinger, 1996).

A separate mechanism by which lava flows grow vertically is inflation, a process that raises the unbroken, solidifying surface of a flow incrementally as the pressure builds from the injection of molten material below the cooled crust (Hon et al., 1994; Hoblitt et al., 2012). Observations of inflating flow fields have shown that the flow propagates laterally by lobes of lava, but before they can solidify as individual lobes, more material is injected beneath the still-intact crust, forming a continuous sub-surface sheet of lava (Hon et al., 1994; Kauahikaua et al., 1998). The gas in the molten interior forms vesicles that become trapped along the bottom surface of the crust, forming vesicle horizons parallel to the solidification front (Cashman and Kauahikaua, 1997). As the solidified crust thickens, and more molten material is injected, a second vesicle layer becomes trapped in the new crust, forming a repeating pattern. Actively inflating flows in Hawai'i have been measured as gaining eight meters of height over the course of twelve weeks (Kauahikaua et al., 1998). Time-lapse photography of these types of flows in Hawai'i show a cyclic, step-wise vertical growth (Hoblitt et al., 2012; Fig. 1, Supplementary Video 1). These flows were only 0.5–1 km wide but are interpreted to be analogous to the expansive flows created in flood basalt eruptions (Self et al., 1996, 1997).

In the Columbia River Flood Basalts and Deccan Traps, evidence of cyclic inflation in the form of bubble horizons are reported in large lava flows up to 50 m thick and with volumes of 100–1000 km^3 (Self et al., 1996). Bubble horizons have been documented in Hawaiian flows several meters in height and with volumes of tens of thousands of cubic meters, also interpreted to represent cycles of inflation (Hon et al., 1994; Cashman and Kauahikaua, 1997; Kauahikaua et al., 1998). In a natural system, many factors could affect the episodic nature of eruptions such as topographic barriers, magma supply rates, or lava tube constriction and dilation; however, the regularity of vesicle horizons seen in many inflated flows suggests that material is not injected at a continuous rate, but possibly in a periodic fashion on relatively short time scales (Hoblitt et al., 2012). As a result, questions are raised:

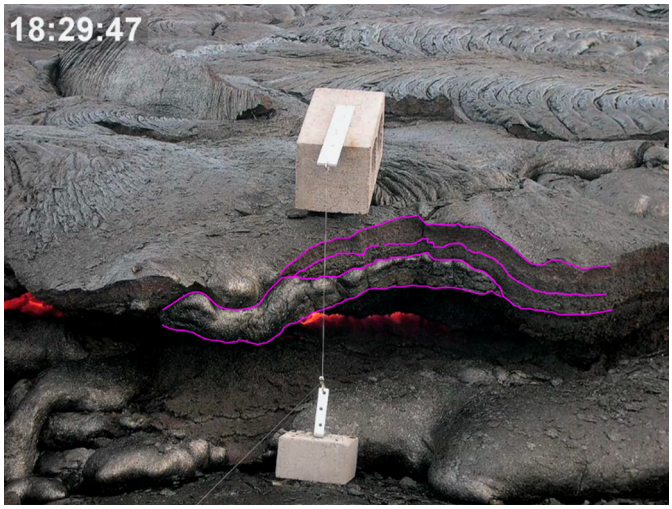

Fig. 1. A still from the Supplemental Video 1 showing an inflating section of a lava flow in Hawai'i (video from supplemental material in Hoblitt et al., 2012). Vertical growth of ~5 cm per pulse is shown in the video. The pink lines indicate old horizontal boundaries between the crust and molten material designated by squeeze-outs of lava or vesicle horizons trapped when the crust first formed. (For interpretation of the references to color in this figure legend, the reader is referred to the web version of this article.)

What eruptive conditions can maintain a coherent crust, but also feed molten material out to the edges of the flow?; and does the regularity of bubble horizons provide information on those conditions? Here we test a mechanism that has been witnessed in active eruptions: pulsating eruption rates (Denlinger, 1997; Patrick et al., 2011; Poland, 2014). We propose that pulsating rates promote inflating lava flows by achieving a balance between faster flow rates which form coherent crust decoupled from a molten core but can also result in rupturing of the crust and resurfacing and lower flow rates that protect coherent crust but can result in stagnation and crust rupture.

1.3. Wax analog experiments

Polyethylene glycol wax (PEG) has been used to simulate volcanic phenomena including channelized flow (e.g., Hallworth et al., 1987; Garry et al., 2006; Cashman et al., 2006), flow over a slope (e.g., Gregg and Fink, 2000; Gregg and Smith, 2003; Lyman and Kerr, 2006), lava domes (e.g., Fink et al., 1993; Fink and Bridges, 1995; Griffiths and Fink, 1997; Buisson and Merle, 2002), compound lava flows (e.g., Blake and Bruno, 2000; Lyman et al., 2005), and preferred pathways and lava tubes (e.g., Griffiths et al., 2003; Anderson et al., 2005), to name a few. The thermomechanical properties of PEG allow it to be a good analog for basaltic lava in particular as it forms a thin viscoelastic crust that eventually becomes brittle upon further cooling (Fig. 2. See also Soule and Cashman, 2004). These previous experiments vary temperature, viscosity, and effusion rate, and incorporate these variables into the non-dimensional number Ψ (cf. paragraphs below and Appendix 1). Analog models of high-silica lava domes showed that aspect ratio, defined as height divided by length, increased with the number of pulses it took to emplace the same volume of material (Fink et al., 1993). Fink et al. (1993), however, did not distinguish between piling up of layers of material and the injection of material beneath the crust. They also used a significantly higher scaled viscosity than is appropriate for basaltic scenarios. Despite being a commonly cited phenomenon in mafic lava flows, inflation has yet to be studied in detail using analog models. In this study, we use PEG 600 wax (Appendix 1) to identify the ideal conditions for maximum inflation potential in a lava flow.

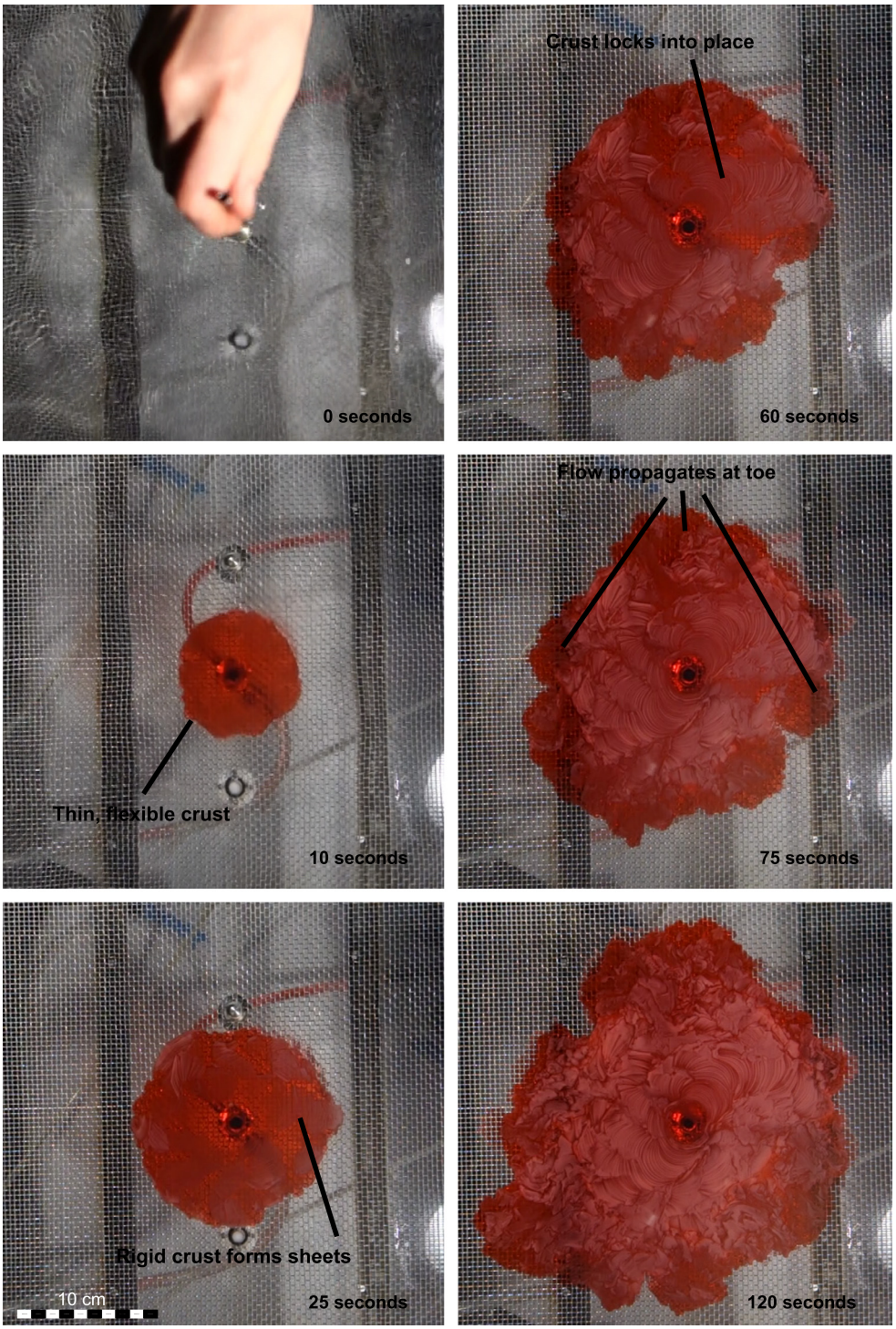

Fig. 2. Progression of experiment PLS15-22 (top view, Ψ – 58.8, P – steady). The wax is dyed red and as the wax cools, an opaque pink crust forms. This sequence shows initial spreading followed by crust seizing up and insulating molten material below it. New wax then breaks out at the edges and the flow grows laterally. Initially, the flow morphology is smooth and sheet like, then ridges begin to form around the vent. The rest of the flow propagates with a pillow-like morphology as the local flow rate decreases due to the increasing area that is being covered.

2. Methods

2.1. Physical parameters

A 60 × 60 × 45 centimeter Plexiglas tank had a hole drilled in the bottom and a metal fixture attached to 15 mm diameter surgical tubing (Fig. 3). A metal wire mesh with 0.5 cm spacing lined the bottom of the tank, to add roughness, similar to the set up used by the group that spearheaded this technique (e.g., Fink and Griffiths, 1990; Griffiths and Fink, 1993; Gregg and Fink, 1995). Clear tubing connected the metal fixture at the base of the tank to the programmable peristaltic Syringe-pump 9000. Peristaltic pumps do produce small pulsations over an otherwise continuous supply of wax, however, these pulsations were visible as only a <1 mm change in height directly over the vent, compared to 2–5 mm changes associated with the imposed pulsations for the experimental conditions presented here. Further,

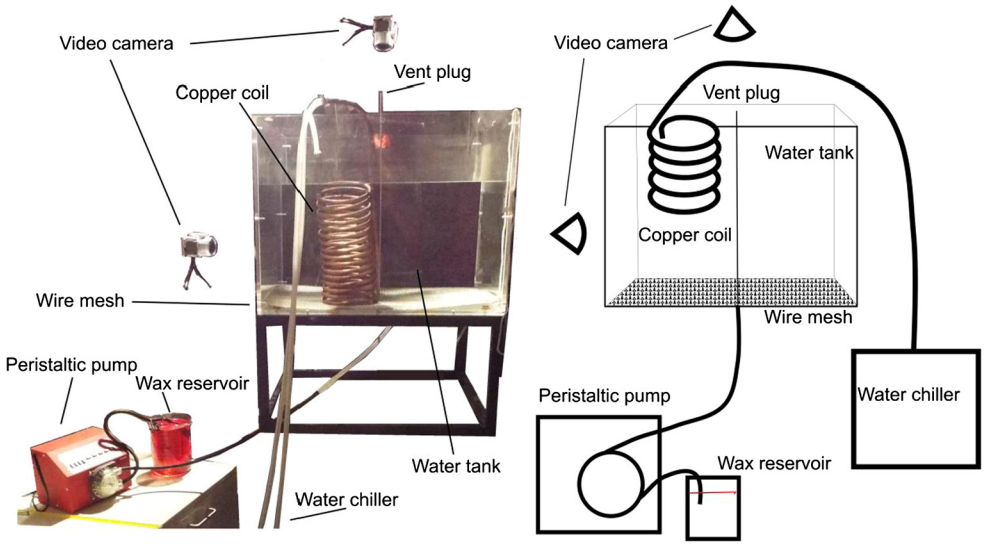

Fig. 3. Experimental set up. A clear cubic tank containing water circulated through a chiller (not shown) and a copper coil inside the tank. Surgical tubing connects the programmable peristaltic pump to the wax reservoir and to the small opening in the bottom of the tank. The tank is lined along the bottom with a 0.5 cm wire mesh and contains a plug for the vent attached to a long rod for easy removal. Multiple cameras were set up to capture each experiment in its entirety from different angles.

these small pulsations were observable only in steady-state experiments with Ψ values over 10, so they are believed to have little to no effect on the data presented in Table 1. Three video cameras were placed around the tank to capture a side, top, and oblique view of each experiment (Supplementary Video 2). PEG 600 wax mixed with food coloring was maintained at a constant temperature (see Table 1 for specific conditions of each experiment) in a 1000 ml beaker suspended in a water bath for the duration of the experiment. The pump was programmed to run at a higher rate (300–450 ml/min) for 10 s, and a subsequent lower rate (50 ml/min) for a time that was varied from experiment to experiment ranging from 10 to 50 s, providing a pulsation interval and magnitude for each experiment. The fluctuating eruption rates were repeated for ~5–10 cycles, until the wax reservoir was emptied or the flow began encroaching on the sides of the tank.

2.2. Scaling

We calculated the non-dimensional value Ψ of each experiment using the equation $\Psi = \Pi\tau_s(\Theta_s)$ which was derived by Fink and Griffiths (1990), and subsequently adjusted by Gregg and Fink (1996). In this equation (Appendix 1), Π is the modified Peclet number, which describes the ratio of heat transfer by diffusion to heat transfer by advection, and $\tau_s(\Theta_s)$ is the characteristic time scale for crust formation. Both are dependent on the parameters and the constants seen in Appendix 1. This scaling factor compares the rate of viscous flow to the rate of crust formation such that Ψ is high when crust formation is much slower than spreading due to gravity (further discussion of the calculation of Ψ can be found in Fink and Griffiths, 1990, 1992; Griffiths and Fink, 1992; and Gregg and Fink, 1996). The Ψ value also incorporates effusion rate (Q), which controls the transfer of heat by advection.

Pulsation intervals are expressed using the scaling factor $P = Q_{avg}/Q_{max}$ where Q_{avg} is the average effusion rate during the entire experiment and Q_{max} is the highest effusion rate during the experiment. This is a useful way to express pulsatory activity because Q_{avg}, which is calculated as total volume divided by total time for the experiments, is a frequently reported value for volcanic eruptions. High values of P correspond to experiments in which the low effusion-rate period was short (e.g., 10 s, fast pulsation), whereas low values of P correspond to experiments in which the low effusion-rate period was long (e.g., 50 s, slow pulsation). These data are presented in Table 1 for all experiments.

2.3. Image processing

Change in plan-view area was calculated every 2 seconds using the program ImageJ from NIH (Abramoff et al., 2004). The proportion of resurfacing was calculated as the area of new material that covered previous crust divided by the area of the previous crust and is calculated after every breakout. The change in height was calculated every 1.25 seconds using the program Tracker Video Analysis and Modeling Tool v. 4.93 (Brown, 2009). Additional editing to merge files, speed up, and change file formatting of video clips was done with Veedub64 and VSDC Free Video Editor (Lee, 2013; VSDC Free Video Editor, 2011).

2.4. Experiment reproducibility

Numerous studies have shown the reproducibility of Ψ value corresponding to morphological changes in surface texture of wax experiments (e.g. Gregg and Fink, 2000; Blake and Bruno, 2000; Garry et al., 2006). We replicated these boundaries in preliminary experiments without modification of effusion rates to confirm that our experimental setup (wax properties, textured bottom of the tank, water temperature) was consistent with previous researchers' setup. Several additional comparisons, shown in Appendix 2, were used to determine the reproducibility of measurement of height using our method. We found that replications were always within 0.25 cm for the final height while inflation heights had a standard deviation between 0.04–0.18 cm, which was an insignificant difference between trials.

3. Results

3.1. Flow parameters

Three wax experiments were erupted with a range of Ψ values from 1.1–58.8 at a steady effusion rate with a single pause in the middle. Eleven experiments had regular pulsation intervals with P values ranging from 0.19 to 0.56, and Ψ values from 1.1 to 13.2 (Table 1). Total flow volumes (V_{tot}) of 500–1530 cm^3 covered areas of 310–860 cm^2 and had final heights of 1.3–3.6 cm.

Table 1
Experimental parameters.

	PLS15-07	PSL15-08	PLS15-09	PLS15-10	PLS15-11	PLS15-12	PLS15-13	PLS15-16	PLS15-18	PLS15-20	PLS15-21	PLS15-15	PLS15-19	PLS15-22
Max Ψ value	8.2	1.1	3.7	8.2	8.1	1.1	3.6	13.2	13.2	4.0	13.2	1.07	13.23	58.79
Min Ψ value	4.8	0.6	2.1	4.8	4.8	0.7	2.1	8.5	8.5	2.9	8.5	–	–	–
P	0.26	0.26	0.29	0.33	0.41	0.56	0.27	0.19[*]	0.44	0.44	0.31	–	–	–
Q_{max} (ml/min)	450	450	450	450	420	420	420	–	300	300	300	300	300	300
Duration (s)	10	10	10	10	10	10	10	–	10	10	10	–	–	–
Q_{min} (ml/min)	50	50	50	50	50	50	50	–	50	50	50	–	–	–
Duration (s)	50	50	40	30	20	10	50	–	20	20	50	–	–	–
Wax temp. (°C)	21	19	20	21	21	19	20	–	22	20	22	–	–	–
Total volume (cm^3)	625	584	650	775	606	705	671	–	540	500	564	535	550	1530
Final area (cm^2)	470	310	460	450	350	540	400	–	460	420	740	440	650	860
Final height (cm)	2.9	3.6	3.3	2.9	2.3	2.0	3.5	–	2.7	2.0	2.0	2.7	2.7	1.3
Area resurfaced (%)	0.23	0.55	0.46	0.20	0.18	0.15	0.26	0.21	0.08	0.17	0.10	0.09	[a]	0.01
Initial morphology	smooth-folds	pillow-rift	pillow-like	folds	smooth-folds	smooth-folds	pillow-like	smooth	smooth	smooth-levee	smooth	pillow-rift	smooth-rift	smooth-folds
Final dominant morphology	pillows with smooth resurfacing	pillows with smooth resurfacing	pillows with folds and resurfacing	pillow-rift	pillow-like	pillow-like	pillows with smooth resurfacing	pillow-like	pillow-rift	pillow-like	pillow-like	pillow-like	rift-pillows	fold-pillows
Aspect ratio	0.142	0.212	0.152	0.124	0.112	0.080	0.173	0.137	0.119	0.122	0.104	0.228	0.188	0.079
Change in height (cm)	0.26	0.27	0.33	0.26	0.10	0.06	0.27	0.37	0.08	0.17	0.19	–	–	–
Lobe height (cm)	0.29	0.57	0.68	0.51	0.58	0.54	0.73	0.52	0.70	0.71	0.65	–	–	–
dx/lobe	0.90	0.47	0.48	0.51	0.16	0.11	0.37	0.72	0.12	0.24	0.30	–	–	–

[*] Value calculated for PLS15-16 with the following flow rates (ml/min in **bold**) and duration of pulse (seconds in *italics*).

rate (ml/min)	**420**	**0**	**300**	**0**	**300**	**50**	**300**	**50**	**300**	**50**	**300**	**50**
duration (s)	*10*	*13*	*10*	*83*	*10*	*50*	*10*	*50*	*10*	*50*	*10*	*35*

[a] No overhead video so resurfacing data could not be determined.

In pulsed experiments, Ψ values fluctuated along with maximum and minimum flow rates and ranged from the lowest set of values at 1.1 (during pulse) and 0.6 (between pulses) (PSL15-08) to the highest set of Ψ values, 13.2 and 8.5 (PLS15-16, 18, and 21). From this point forward, experiments are compared by maximum Ψ value for simplicity. The experiments with pulsating eruption rates had P values of 0.19–0.56 with higher values corresponding to faster pulsation rates and shorter time spent at lower effusion rates. Upon the initiation of the higher effusion rate within a pulse, the flow top rose by 1.1–3.9 mm on average, and was followed by a slight decrease of 0.6–2 mm as hydraulic pressure ebbed during lower effusion, resulting in the overall change in height shown in Table 1. One experiment, PLS15-16, did not follow the typical pattern of intervals initially; however, as the majority of the run did have regular pulses in eruption rate, it is included in the study. The duration of each eruption rate in each experiment is reported in Table 1.

3.2. Flow morphology

All experiments initially produced the morphological type associated with the maximum Ψ value as defined by Fink and Griffiths (1990) and refined by Gregg and Fink (1996) (pillows < 0.65; 0.65–2.8 rifts; 2.8–6.4 folds; >6.4 smooth with eventual levees). Steady effusion rate experiments sustained the initial morphology for a longer period than pulsed experiments, but eventually, even in the steady experiments, lobes formed around the edges as the local effusion rate and Ψ value decreased due to the broader flow front being supplied by the same effusion rate. Shortly after a reduction in flow rate in pulsed experiments, new crust tended to form with a pillow-like morphology, regardless of the Ψ value at the vent and flow propagation was typically limited to breakouts along the flow front (Table 1). Subsequent increases in flow rate during these pulsed experiments produced areas of breakout, either at the edge of the flow, at cracks close to the vent, or both. These areas of breakout had crust consistent with high Ψ values, such as rifts, suggesting high coupling between crust and core. Initially, the pulsed source produced flows with concentric bands of different surface morphologies. However, as the flow field evolved, the boundaries between these bands became harder to distinguish (Fig. 4). Flows that propagated primarily at the edge of the flow had greater perimeters, resulting in rings with progressively thinner bands (as viewed from above) and lower local effusion rates. The predominant morphology became pillow-like similar to steady-effusion experiments (e.g., PLS15-20, PLS15-12, Fig. 4) as these flow fields continued to evolve. Conversely, flows that had breakouts on the top surface, as opposed to the margins, had high percentages of resurfacing. In these cases, the flow produced smooth morphologies overtopping older pillows (e.g., PLS15-08, PLS15-13, Fig. 5).

3.3. Lateral and vertical flow progression

Shortly after both pulsating and steady-state eruptions started, crust started forming and stagnating as wax entered the cold water, hardening and freezing in place while the fluid material underneath continued to the active edge of the flow (Fig. 2, Supplemental Video 3). The formation of a coherent crust locked in place promoted lateral progression in both types of experiments, however, the rate of this progression was faster for steady effusion rates and higher Ψ values. Flows at steady effusion rate tended to spread laterally and obtain a consistent height shortly after experiment initiation, which changed only when there was a pause in supply (Fig. 6). In contrast, pulsating effusion rates resulted in lateral progression, but also incremental vertical growth (Fig. 7). For pulsed experiments, lateral and vertical growth was greatest shortly after the start of a higher effusion rate pulse and decreased during the phase of lower effusion rate (Fig. 8). Rapid pulsation (high P) always resulted in more extensive lateral growth than lower P experiments, regardless of Ψ value (Fig. 8). The aspect ratio of the flows dropped by more than half (0.212 to 0.080, Table 1) when the frequency of pulsation doubled. Final aspect ratios of steady-effusion rate experiments should only be used qualitatively in comparison to pulsating experiments as they all were affected by the long pauses in each experiment, resulting in higher ratios than would be expected had there not been a pause. The effect of lower P values, higher vertical growth and higher aspect ratios, is illustrated by experiments PLS15-08 and PLS15-12 which have the same Ψ value of approximately 1.1 but different P values, 0.26 and 0.56, respectively (Fig. 8). Even though all experiments experienced vertical growth, the mechanism by which they thickened was different, as discussed in the next section.

3.4. Inflation and resurfacing

Vertical growth occurred by two mechanisms: inflation and resurfacing. Resurfacing is defined as vertical growth of a flow by the addition of new layers on top of the old crust. Lower P and lower Ψ values favored resurfacing, which predominantly occurred when the onset of the higher effusion rate ruptured the crust. New cracks in the surface tended to be filled with fresh wax or be squeezed closed during deflation. This kind of vertical growth resulted in distinct lobes piled together as new lobes flowed on top of older lobes. Distinguishing the component of vertical growth due to resurfacing and inflation in each experiment was done visually so that the two could be quantified separately.

Inflation was observed in this study by the rising of a coherent crust as new material was injected below the crust's surface. In experiments that inflated, the vertical growth occurred at the onset of the higher effusion rate phase and continued until the crust ruptured, predominantly at the edge, seen as a slight period of deflation in the height profiles and surges in the area profiles of the experiments (Table 1, Fig. 8). Inflation only occurred when a sufficiently strong and coherent crust provided resistance to breakouts and allowed internal pressure to rise. This required condition for inflation tended to be met for high Ψ value experiments when P was low (slow pulsation). In low Ψ value experiments, rapid pulsation was required to promote inflation and prevent resurfacing. As experiments progressed, the ability to grow vertically by inflation decreased. Longer intervals between pulses (higher P) and lower Ψ values positively correlated with greater magnitude of inflation and deflation per pulse, and in a greater increase from initial to final height (Table 1). To normalize for any contribution to change in height from temperature and viscosity as opposed to effusion rate (which are all contained in the Ψ value calculation) the increment of inflation was divided by the height of an initial lobe to give a non-dimensional inflation efficiency number (Table 1).

4. Discussion

From this work we can make several general statements about the emplacement dynamics of wax analog experiments and lava flow fields. Eruptions with steady effusion rates are capable of extensive areal coverage, but typically do not build up vertically as the continual flow of lava does not allow the crust at the perimeter to stagnate, thereby preventing build up of the internal pressure necessary for inflation. Lower effusion rates result in rapid crust formation that causes quench rinds to form between flow lobes. These lobes commonly pile up on top of each other, driving vertical growth by resurfacing but with little lateral progression. However, by pulsating the effusion rates of wax eruptions in a controlled setting, we achieved conditions that appeared to promote surface

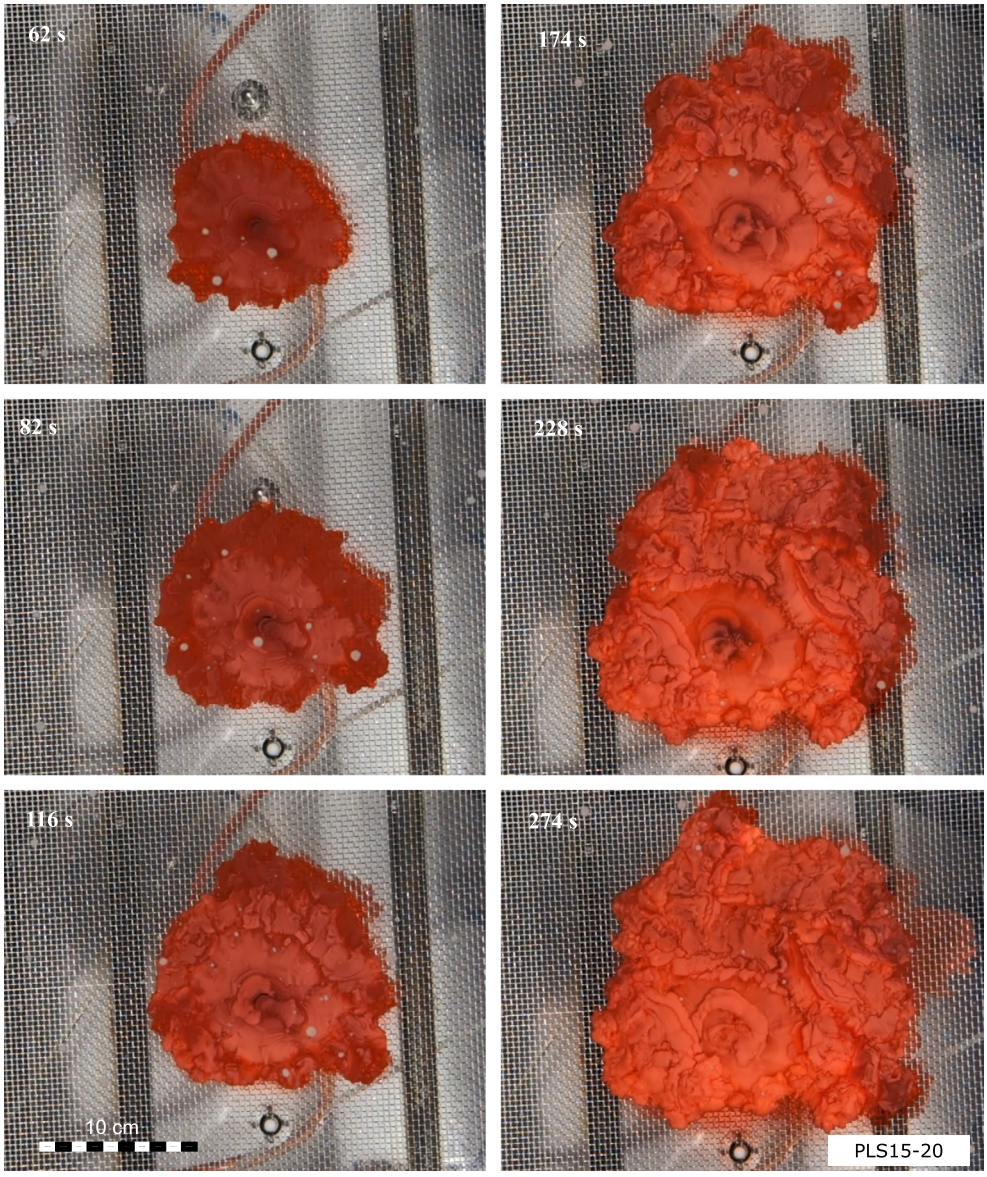

Fig. 4. Progression of experiment PLS15-20 (Ψ – 4, P – .44) which grew primarily through breakouts along the margins due to a moderate pulsation rate (high P). The first image in the upper left hand corner shows the initial high effusion rate, leading to a smooth morphology. The image below shows the 2nd pulse, which shows a small amount of resurfacing right at the vent but primarily a ring of material breaking out along the edges with fairly smooth morphology. The third image shows the third pulse, which begins to show a pillow-like morphology. The second column of images shows further lateral progression of the flow. The morphology becomes lumpier and some resurfacing is also seen along cracks between pulse 1 and pulse 2 crust.

crustal thickening as well as lateral transport of sub-crustal wax. This process presents a feasible mechanism for inflation in large lava fields, by promoting propagation via lobes at the far edges of the flow.

4.1. Eruption tempo: the effect of pulsation on flow morphology

Previous studies on Ψ value and morphology of wax flows have primarily focused on simple flows immediately adjacent to the vent as the experiments were run only long enough for an initial morphology to develop (e.g., Fink and Griffiths, 1990, 1992, 1998; Gregg and Fink, 1995, 1996, 2000). Findings of Gregg and Keszthelyi (2004) show that basaltic crust formation at great distances from the vent is dependent on the local effusion rate, which can be highly variable in a natural setting. With this study's longer-duration experiments and more extensive flow fields, the morphology depended strongly on the local effusion rate wherever the wax was breaking out from the crust. The pattern of pulsation in our experiments created rapid local effusion rates, which resulted in smooth morphologies initially. However, upon the release of pressure inside the flow, morphologies returned to lumpy and pillow-like regardless of the effusion rate at the vent.

The tempo of pulsating effusion rates affects the surface morphology as well as the areal extent and final thickness of the flow with slower pulsation creating flows with higher aspect ratios, due to resurfacing and inflation. Rapid pulsation prevented the crust at the edge of a flow from solidifying, decreasing inflation and leading to breakouts around the base of the flow front, as opposed to emanating from cracks on the surface. Similarly, flows with high Ψ values were not able to form thick crusts capable of building up pressure, which creates longer runouts and little vertical growth. We discovered that pairing an intermediate pulse interval (P between 0.3–0.4) with a moderate eruption rate (Ψ value of 3 to 11, and given a reasonable temperature range) maximizes vertical growth while also preserving extensive and continued lateral growth (Fig. 9). The decrease in eruption rate during the low point

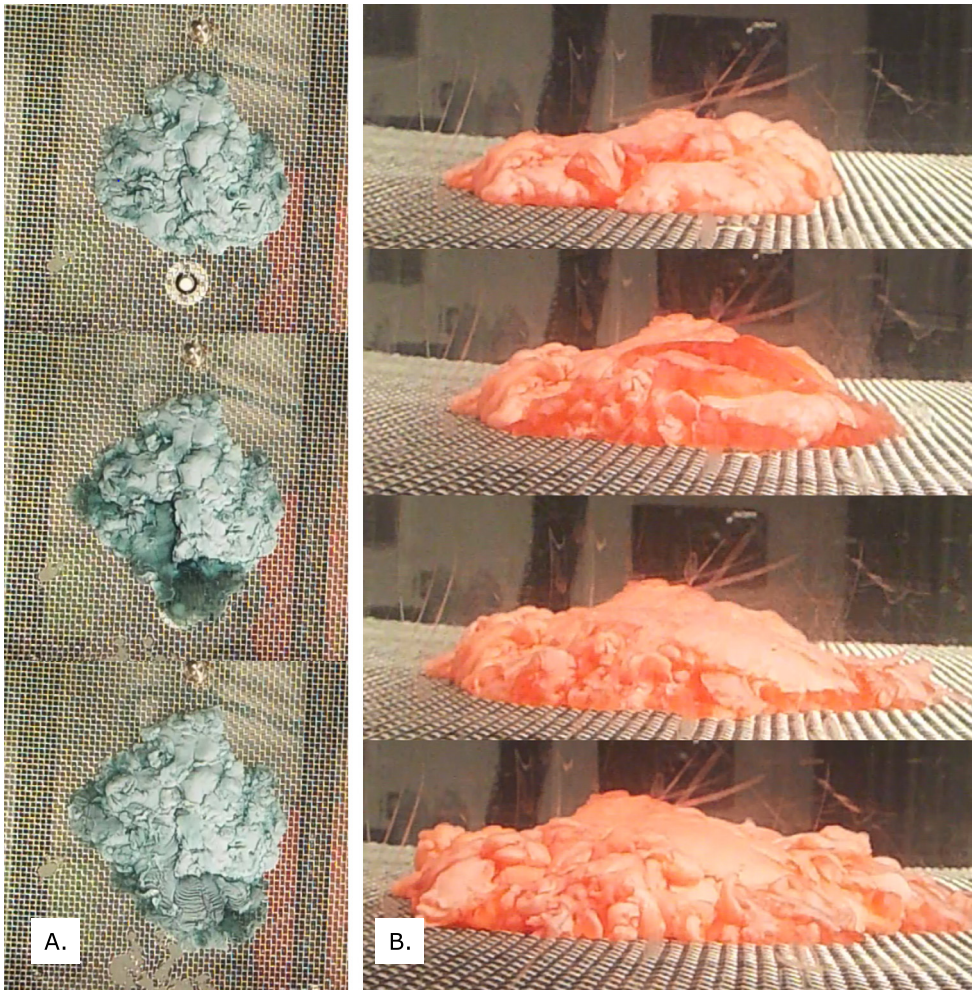

Fig. 5. Images of two experiments both illustrating high degrees of resurfacing. A. Top view of PLS15-09 (Ψ – 3.7, P – 0.29) with an initial pillow-like morphology that is overrun with a breakout in the second frame. That breakout forms ridges as the local Ψ value was increased due to a buildup of pressure during the low effusion rate phase, which can be seen more clearly in the third panel after the crust has solidified. B. Side view of experiment PLS15-08 (Ψ – 1.1, P – 0.26) shows a lumpy crust being resurfaced by a smooth morphology. This mechanism increases the height of a lava flow without the process of inflation.

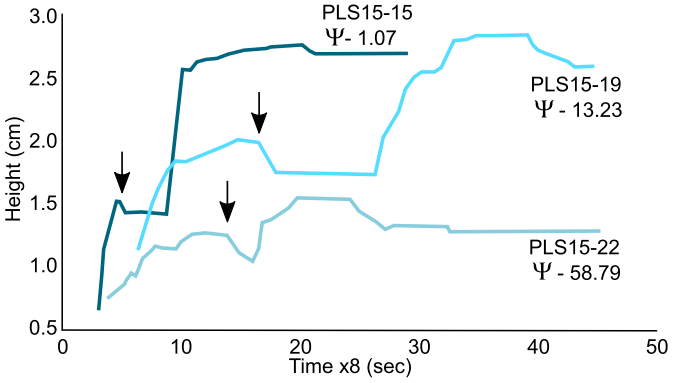

Fig. 6. Height profiles over time of three steady effusion rate experiments with differing Ψ value. Each experiment shows a jog indicated by arrows where the pump was paused temporarily. After a quick rise in height, the wax flows would remain at that height and expand laterally. These experiments had P values approaching 1.

in a pulse allows for the surface crust to thicken, which insulates molten interior lava as well as provides a rigid network of pathways that can transport this material to the distal portions of the flow.

4.2. Hawaiian inflation and resurfacing

The most studied locality of active inflation of a flow field is Kīlauea volcano in Hawai'i (Hon et al., 1994; Kauahikaua et al., 1998; Hoblitt et al., 2012). Flow fields from the years 1988–1990 showed inflation of two meters over five days (Hon et al., 1994) and 9.5 m over ~30 days (Kauahikaua et al., 1998). The eruptive state at the vent was periodic during this time with pauses from 1–4 days, however, it is not stated if this pulsation occurred during the emplacement of these specific lava flows (Mangan et al., 1995). The change in height in the flow field was rapid in the beginning, and then began to decrease as the crust thickened, the flow grew in area, and more pressure and larger volume of material was needed to lift the entire crust. This is the same pattern we observed in our experiments, which suggests that episodic source conditions could produce extended periods of inflation, allowing for greater overall heights within a single flow unit. In the Hawai'i flows, the supply rate to the perimeter of the lava is reported as time-averaged values (Q_{avg}); however, they were reported to have decreased over the course of 5 hours from 1.1 m^3/s to 0.3 m^3/s, which would be equivalent to Ψ values of 13 to 9.4 (using the method and values of $\Delta\rho = 1400$, $t_s = 10$, and $\eta = 10000$ in Gregg and Keszthelyi, 2004). A photograph of a cross-section through the cooled and solidified inflated flow shows banding associated with

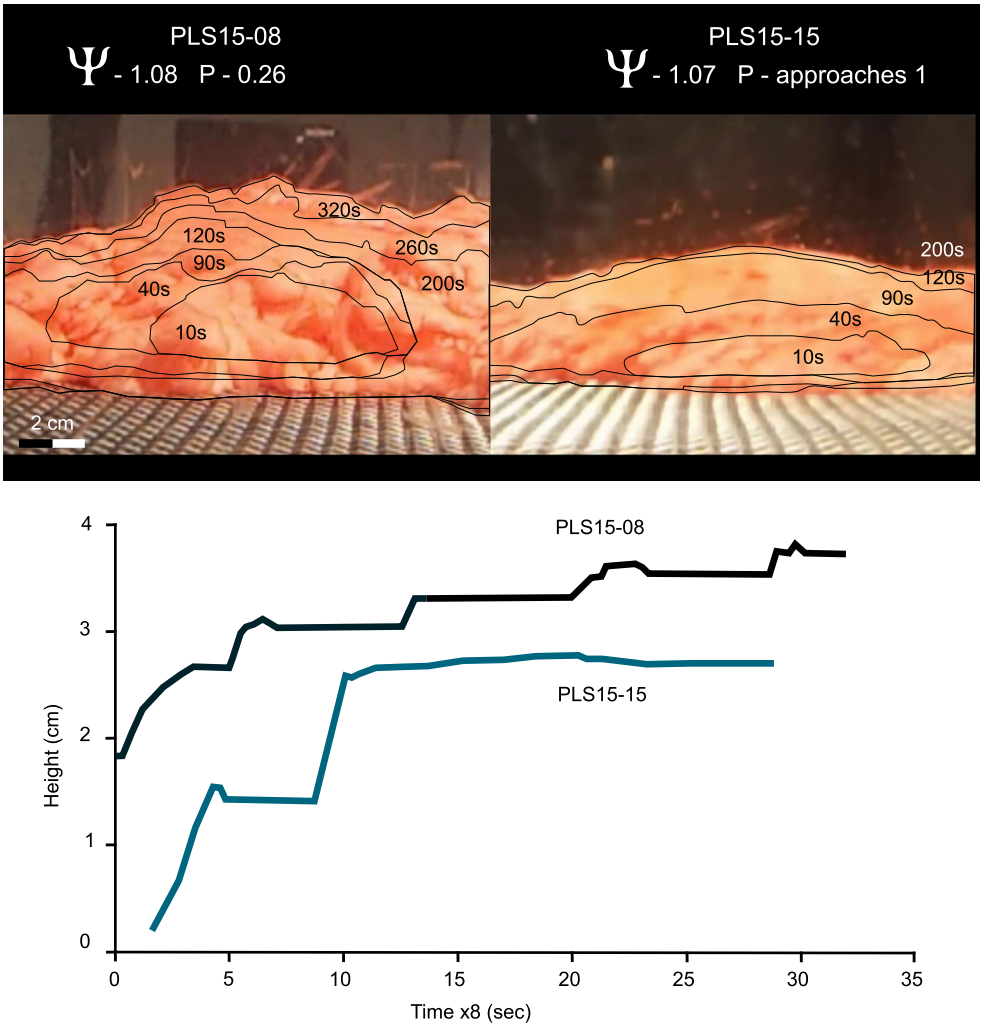

Fig. 7. Photo and chart of the height vs time showing the effect of a pulsating effusion rate. Experiments have the same Ψ value, but PLS15-15 (V_{tot} 535 cm^3) had a steady effusion rate with a single pause while PLS15-08 (V_{tot} 584 cm^3) had 50-second between high effusion rate pulses. Thin black lines show the outline of the lava flow at each time, illustrating the ability of the pulsed experiment to reach greater height than the steady eruption.

incremental increases in height of about 5 cm to 8 cm and an original lobe height of 30 cm (Hon et al., 1994, Fig. 4c, scale as in caption). Calculating the increment of inflation divided by the original lobe height gives us values of 0.16–0.26, which, along with the Ψ values of 9.4 to 13 reported above, can be compared to experimental data on Fig. 9, where the dashed red line gives inflation increment and the blue dashed line is the percent area resurfaced. This particular lava flow plots within the region of efficient inflation, with P ranging from 0.4 to 0.5 (checkered zone). Given these P values and the reported Q_{avg} values of 0.3–1.1 m^3/s, we calculate Q_{max} to be 3.1 m^3/s. If we assume that the eruption was emplaced by a pulsating source with approximately constant frequency, we suggest that the flow experienced effusion rates 3× as high as the measured average. This method currently does not allow us to constrain the minimum eruption rate and our experiments did not vary this factor so a frequency of the pulsation cannot be estimated.

Episodic local injections of material without prolonged pauses seem to be necessary to maintain an inflating crust for more than a few days. For Hawaiian-sized eruptions, flow rates that fluctuate between 1 and 3 m^3/s could account for the inflation seen on the coastal plains which reached ∼10 m over the course of ∼4 weeks before it was resurfaced (Kauahikaua et al., 1998).

5. Conclusion

Important eruption parameters, such as effusion rate and tempo, may control the environmental impact of large eruptions. Thus, it is valuable to link effusion rate and eruption tempo of large lava fields to the characteristics of preserved volcanic products, such as flow morphology. Here we have shown that one of the most common lava emplacement mechanisms, inflation, appears to be enhanced by pulsations in effusion rates. Inflation requires a coherent solid crust, a widespread molten core, and a supply of magma to sustain the inflation. In wax experiments, punctuating intervals of low instantaneous effusion rates with short pulses of high flux produced the conditions required for inflation, and enhanced transport of molten material to the edges of the flow field. Furthermore, such pulsating eruption rates provide conditions that favor inflation over resurfacing, which suggests the aspect ratio of ancient basaltic lava flows on Earth as well as other planets are controlled, in part, by the eruption tempo.

Lava flows record the sequential nature of inflation with repeated vesicle horizons and horizontal ridges visible along vertical cracks that penetrate thick flows (e.g., Cashman and Kauahikaua, 1997). These features preserve the increment of inflation that occurred during emplacement. Combined with the results of the ex-

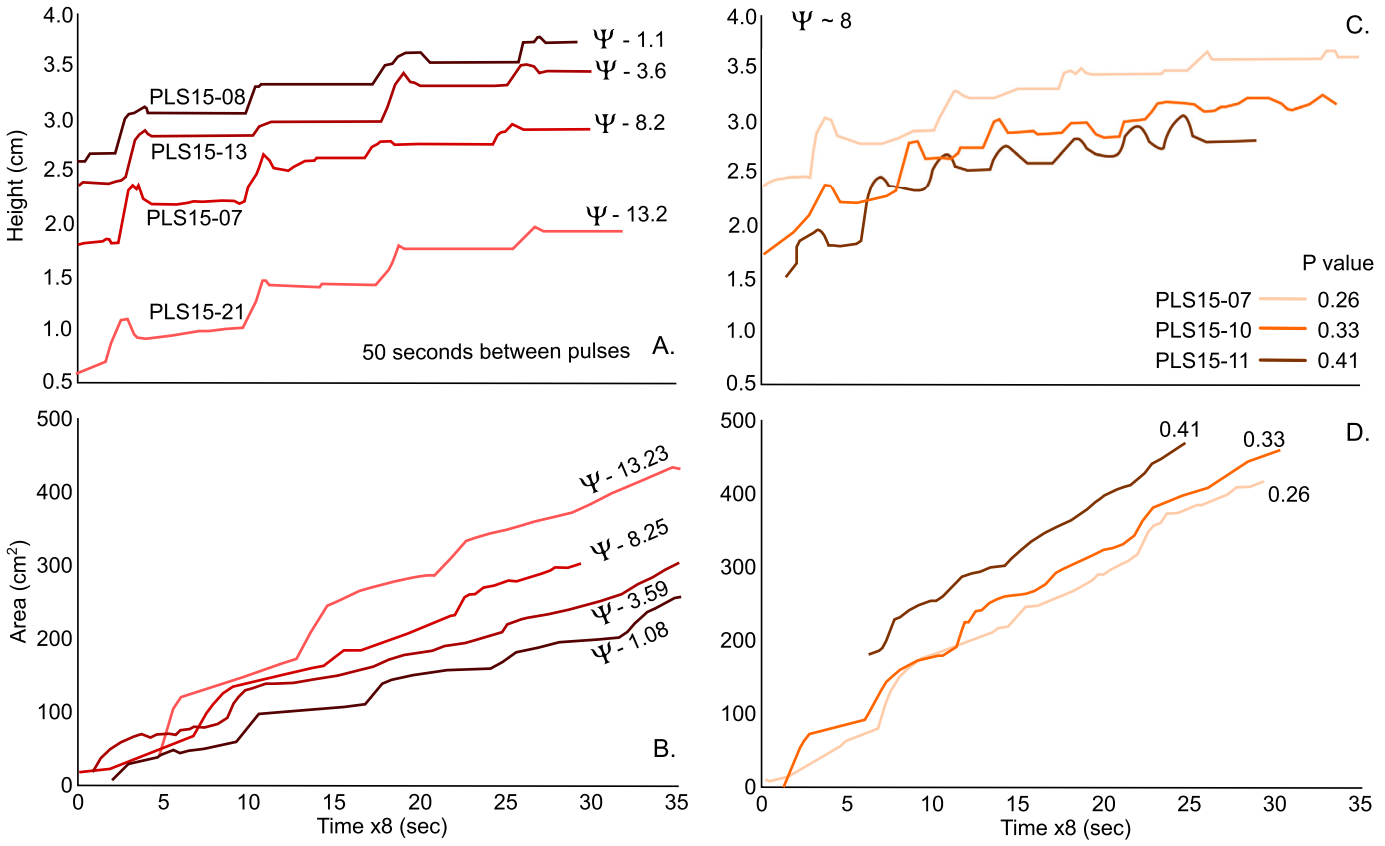

Fig. 8. Change in height (A) and area (B) of experiments with different Ψ values. Lower Ψ value corresponds to higher viscosity and slower effusion rate, which results in faster vertical growth and more modest lateral growth. All experiments have similar pulsation rates of 50 s between pulses. Change in height (C) and area (D) with time for experiments of similar Ψ value but different pulsation rates (P value). As pulsation rates increase (high P), the rate of change in flow height decreases while the rate of change of flow area increases. Adding additional time for the crust to form between pulses (lowering P) allows flows to build up a stronger crust which can resist more force, resulting in greater inflation. Note that SLP07 is present on all four panels (Ψ – 8.25, P – 0.26).

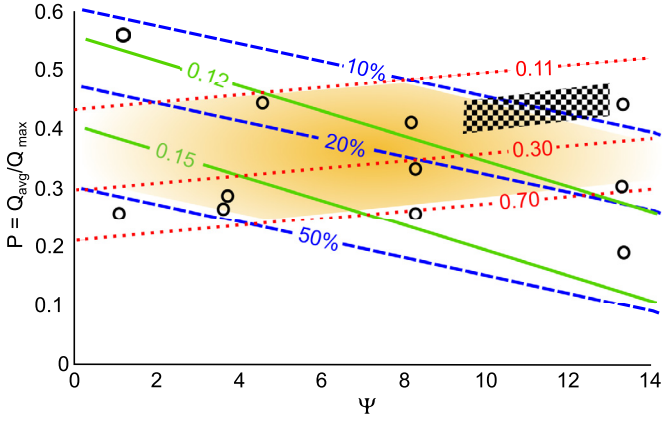

Fig. 9. Regime diagram showing the effect of Ψ value and P value on the ability of a flow to grow by inflation. As Ψ value and P value increase, the percentage of resurfacing decreases, but so does the aspect ratio. More material is being pushed to the edges of the flow as opposed to building up the height. Individual experiments are black empty circles. Blue dashed lines indicate percent resurfacing by area; green lines represent final aspect ratio of the flow; red dashed lines represent normalized change in flow height. The orange shaded region is where the most efficient inflation can occur. The checkered region is where one of the observed inflating flows from 1988 at Kīlauea plots, data from Hon et al. (1994). (For interpretation of the references to color in this figure legend, the reader is referred to the web version of this article.)

periments presented here, these field measurements can be used to constrain effusion rate and tempo. We present an example of the utility of our new framework for a well-documented lava flow in Hawai'i. We estimate that an inflating flow in Hawai'i that had an average eruption rate of 1.1 m^3/s may have had instantaneous rates as high as 3.1 m^3/s to achieve the observed growth.

Acknowledgements

This research was funded by U.S. National Science Foundation grant EAR-1250440. The authors would also like to thank John Fink and Steve Anderson for their insights on PEG wax experiments and Alex Sehlke for viscosity discussions. Major support in running the experiments was provided by Sean Peters. The manuscript

was greatly improved thanks to comments by Tracy Gregg and an anonymous reviewer.

Appendix A. Supplementary material

Supplementary material related to this article can be found online at http://dx.doi.org/10.1016/j.epsl.2017.08.016.

References

Abramoff, M.D., Magalhaes, P.J., Ram, S.J., 2004. Image Processing with ImageJ. Biophotonics International 11, 36–42.

Anderson, S.W., McColley, S.M., Fink, J.H., Hudson, R.K., 2005. The development of fluid instabilities and preferred pathways in lava flow interiors: insights from analog experiments and fractal analysis. Spec. Pap., Geol. Soc. Am. 396, 147–161.

Anderson, S.W., Stofan, E.R., Smrekar, S.E., Guest, J.E., Wood, B., 1999. Pulsed inflation of pahoehoe lava flows: implications for flood basalt emplacement. Earth Planet. Sci. Lett. 168 (1), 7–18.

Black, B.A., Manga, M., 2017. Volatiles and the tempo of flood basalt magmatism. Earth Planet. Sci. Lett. 458 (1), 130–140.

Blake, S., Bruno, B.C., 2000. Modelling the emplacement of compound lava flows. Earth Planet. Sci. Lett. 184 (1), 181–197.

Brown, D., 2009. Video modeling and tracker. In: AAPT Topical Conference: Computer Modeling in the Introductory Course. AAPT Summer Meeting.

Buisson, C., Merle, O., 2002. Experiments on internal strain in lava dome cross sections. Bull. Volcanol. 64 (6), 363–371.

Cañón-Tapia, E., Coe, R., 2002. Rock magnetic evidence of inflation of a flood basalt lava flow. Bull. Volcanol. 64 (5), 289–302.

Cañón-Tapia, E., Walker, G.P.L., Herrero-Bervera, E., 1997. The internal structure of lava flows—insights from AMS measurements II: Hawaiian pahoehoe, toothpaste lava and 'a'ā. J. Volcanol. Geotherm. Res. 76 (1), 19–46.

Cashman, K.V., Kauahikaua, J.P., 1997. Reevaluation of vesicle distributions in basaltic lava flows. Geology 25 (5), 419–422.

Cashman, K.V., Kerr, R.C., Griffiths, R.W., 2006. A laboratory model of surface crust formation and disruption on lava flows through non-uniform channels. Bull. Volcanol. 68 (7–8), 753–770.

Cashman, K.V., Thornber, C., Kauahikaua, J.P., 1999. Cooling and crystallization of lava in open channels, and the transition of Pāhoehoe Lava to 'A'ā. Bull. Volcanol. 61 (5), 306–323.

Castruccio, A., Rust, A.C., Sparks, R.S.J., 2013. Evolution of crust- and core-dominated lava flows using scaling analysis. Bull. Volcanol. 75 (1), 1.

Courtillot, V., Fluteau, F., 2014. A review of the embedded time scales of flood basalt volcanism with special emphasis on dramatically short magmatic pulses. Spec. Pap., Geol. Soc. Am. 505. SPE505-15.

Denlinger, R.P., 1997. A dynamic balance between magma supply and eruption rate at Kilauea volcano, Hawaii. J. Geophys. Res., Solid Earth 102 (B8), 18091–18100.

Duraiswami, R.A., Dole, G., Bondre, N., 2003. Slabby pahoehoe from the western Deccan Volcanic Province: evidence for incipient pahoehoe–aa transitions. J. Volcanol. Geotherm. Res. 121 (3), 195–217.

Fink, J.H., Bridges, N.T., 1995. Effects of eruption history and cooling rate on lava dome growth. Bull. Volcanol. 57 (4), 229–239.

Fink, J.H., Bridges, N.T., Grimm, R.E., 1993. Shapes of Venusian "pancake" domes imply episodic emplacement and silicic composition. Geophys. Res. Lett. 20 (4), 261–264.

Fink, J.H., Griffiths, R.W., 1990. Radial spreading of viscous-gravity currents with solidifying crust. J. Fluid Mech. 221, 485–509.

Fink, J.H., Griffiths, R.W., 1992. A laboratory analog study of the surface morphology of lava flows extruded from point and line sources. J. Volcanol. Geotherm. Res. 54 (1–2), 19–32.

Fink, J.H., Griffiths, R.W., 1998. Morphology, eruption rates, and rheology of lava domes: insights from laboratory models. J. Geophys. Res., Solid Earth 103 (B1), 527–545.

Garry, W.B., Gregg, T.K., Soule, S.A., Fornari, D.J., 2006. Formation of submarine lava channel textures: insights from laboratory simulations. J. Geophys. Res., Solid Earth 111 (B3), B03104. http://dx.doi.org/10.1029/2005JB003796.

Gregg, T.K., Fink, J.H., 1995. Quantification of submarine lava-flow morphology through analog experiments. Geology 23 (1), 73–76.

Gregg, T.K., Fink, J.H., 1996. Quantification of extraterrestrial lava flow effusion rates through laboratory simulations. J. Geophys. Res., Planets 101 (E7), 16891–16900.

Gregg, T.K., Fink, J.H., 2000. A laboratory investigation into the effects of slope on lava flow morphology. J. Volcanol. Geotherm. Res. 96 (3), 145–159.

Gregg, T.K., Keszthelyi, L.P., 2004. The emplacement of pahoehoe toes: field observations and comparison to laboratory simulations. Bull. Volcanol. 66 (5), 381–391.

Gregg, T.K., Smith, D.K., 2003. Volcanic investigations of the Puna Ridge, Hawai'i: relations of lava flow morphologies and underlying slopes. J. Volcanol. Geotherm. Res. 126 (1), 63–77.

Griffiths, R.W., Fink, J.H., 1992. Solidification and morphology of submarine lavas: a dependence on extrusion rate. J. Geophys. Res., Solid Earth 97 (B13), 19729–19737.

Griffiths, R.W., Fink, J.H., 1993. Effects of surface cooling on the spreading of lava flows and domes. J. Fluid Mech. 252, 667–702.

Griffiths, R.W., Fink, J.H., 1997. Solidifying Bingham extrusions: a model for the growth of silicic lava domes. J. Fluid Mech. 347, 13–36.

Griffiths, R.W., Kerr, R.C., Cashman, K.V., 2003. Patterns of solidification in channel flows with surface cooling. J. Fluid Mech. 496, 33–62.

Hallworth, M.A., Huppert, H.E., Sparks, R.S.J., 1987. Lava flows. Mod. Geol. 11, 93–107.

Hoblitt, R.P., Orr, T.R., Heliker, C., Denlinger, R.P., Hon, K., Cervelli, P.F., 2012. Inflation rates, rifts, and bands in a pāhoehoe sheet flow. Geosphere 8 (1), 179–195.

Hon, K., Kauahikaua, J., Denlinger, R., Mackay, K., 1994. Emplacement and inflation of pahoehoe sheet flows: observations and measurements of active lava flows on Kilauea Volcano, Hawaii. Geol. Soc. Am. Bull. 106 (3), 351–370.

Kauahikaua, J., Cashman, K.V., Mattox, T.N., Heliker, C.C., Hon, K.A., Mangan, M.T., Thornber, C.R., 1998. Observations on basaltic lava streams in tubes from Kilauea Volcano, island of Hawai'i. J. Geophys. Res., Solid Earth 103 (B11), 27303–27323.

Keszthelyi, L., Denlinger, R., 1996. The initial cooling of pahoehoe flow lobes. Bull. Volcanol. 58 (1), 5–18.

Lee, A., Oct. 27th, 2013. VeeDub64. Computer software. VirtualDub. Vers. 1.10.4. http://virtualdub.sourceforge.net/. Web. 4 Aug. 2016.

Lyman, A.W., Kerr, R.C., 2006. Effect of surface solidification on the emplacement of lava flows on a slope. J. Geophys. Res., Solid Earth 111 (B5).

Lyman, A.W., Kerr, R.C., Griffiths, R.W., 2005. Effects of internal rheology and surface cooling on the emplacement of lava flows. J. Geophys. Res., Solid Earth 110 (B8).

Mangan, M.T., Heliker, C.C., Mattox, T.N., Kauahikaua, J.P., Helz, R.T., 1995. Episode 49 of the Pu'u'O'o-Kupaianaha eruption of Kilauea volcano-breakdown of a steady-state eruptive era. Bull. Volcanol. 57 (2), 127–135.

Moore, J.G., 1975. Mechanism of formation of pillow lava: pillow lava, produced as fluid lava cools underwater, is the most abundant volcanic rock on earth, but only recently have divers observed it forming. Am. Sci. 63 (3), 269–277.

Patrick, M.R., Orr, T., Wilson, D., Dow, D., Freeman, R., 2011. Cyclic spattering, seismic tremor, and surface fluctuation within a perched lava channel, Kīlauea Volcano. Bull. Volcanol. 73 (6), 639–653.

Peterson, D.W., Tilling, R.I., 1980. Transition of basaltic lava from pahoehoe to aa, Kilauea Volcano, Hawaii: field observations and key factors. J. Volcanol. Geotherm. Res. 7 (3), 271–293.

Pinkerton, H., James, M., Jones, A., 2002. Surface temperature measurements of active lava flows on Kilauea volcano, Hawai'i. J. Volcanol. Geotherm. Res. 113 (1), 159–176.

Poland, M.P., 2014. Time-averaged discharge rate of subaerial lava at Kīlauea Volcano, Hawai'i, measured from TanDEM-X interferometry: implications for magma supply and storage during 2011–2013. J. Geophys. Res., Solid Earth 119 (7), 5464–5481.

Reidel, S.P., Camp, V.E., Tolan, T.L., Martin, B.S., 2013. The Columbia River flood basalt province: stratigraphy, areal extent, volume, and physical volcanology. Spec. Pap., Geol. Soc. Am. 497, 1–43.

Rowland, S.K., Walker, G.P., 1990. Pahoehoe and aa in Hawaii: volumetric flow rate controls the lava structure. Bull. Volcanol. 52 (8), 615–628.

Self, S., Thordarson, T., Keszthelyi, L., 1997. Emplacement of continental flood basalt lava flows. In: Mahoney, J.J., Coffin, M.F. (Eds.), Large Igneous Provinces: Continental, Oceanic, and Planetary Flood Volcanism. In: Geophys. Monogr., vol. 100, pp. 381–410.

Self, S., Thordarson, T., Keszthelyi, L., Walker, G.P.L., Hon, K., Murphy, M.T., Long, P., Finnemore, S., 1996. A new model for the emplacement of Columbia River basalts as large, inflated pahoehoe lava flow fields. Geophys. Res. Lett. 23 (19), 2689–2692.

Soule, S.A., Cashman, K.V., 2004. The mechanical properties of solidified polyethylene glycol 600, an analog for lava crust. J. Volcanol. Geotherm. Res. 129 (1), 139–153.

Tobin, T.S., Bitz, C.M., Archer, D., 2017. Modeling climatic effects of carbon dioxide emissions from Deccan Traps Volcanic Eruptions around the Cretaceous–Paleogene boundary. Palaeogeogr. Palaeoclimatol. Palaeoecol. 478, 139–148. http://dx.doi.org/10.1016/j.palaeo.2016.05.028.